3-3.6 GHz Wideband GaN Doherty power amplifier exploiting output compensation stages

3–3.6 GHz wideband GaN Doherty power amplifier exploiting output compensation stages

Jorge Moreno Rubio, Jie Fang, Vittorio Camarchia, *Member, IEEE*, Roberto Quaglia, Marco Pirola *Member, IEEE*, and Giovanni Ghione *Fellow, IEEE*

***Abstract*—We discuss the design, realization and experimental characterization of a GaN-based hybrid Doherty power amplifier for wideband operation in the 3–3.6 GHz frequency range. The design adopts a novel, simple approach based on wideband compensator networks. Second-harmonic tuning is exploited for the main amplifier at the upper limit of the frequency band, thus improving gain equalization over the amplifier bandwidth. The realized amplifier is based on a packaged GaN HEMT, and shows, at 6 dB of output power back-off, a drain efficiency higher than 38 % in the 3–3.6 GHz band, gain around 10 dB, and maximum power between 43 dBm and 44 dBm, with saturated efficiency between 55 % and 66 %. With respect to the state of the art, we obtain, at a higher frequency, a wideband amplifier with similar performances in terms of bandwidth, output power, and efficiency, through a simpler approach. Moreover, the measured constant maximum output power of 20 W suggests that the power utilization factor of the 10 W (Class A) GaN HEMT is excellent over the amplifier band.**

***Index Terms*—Wideband microwave amplifiers, broadband matching networks, Doherty power amplifiers, GaN-based FETs, WiMAX**

I. Introduction

THE success of the Doherty power amplifier [1] for the implementation of wireless base-stations is mainly related to its high efficiency in presence of modulated signals with high ratio between peak and average power, i.e. non-constant envelope [2]. In fact, because of its high efficiency over a wide range of power levels, Doherty amplifiers can effectively handle non-constant envelope signals without additional external controls [3], [4] that negatively impact on the overall system complexity, size, and efficiency. Limitations in linearity and bandwidth are recognized to be the most important Doherty amplifier issues; concerning the first point, several linearization strategies, able to comply with the stringent communication system requirements, have been successfully reported [5]–[7]. Regarding instead bandwidth limitations, the rather low fractional bandwidth value (typically less than 10 %) of the conventional Doherty power amplifier prevents its exploitation in multi-band, multi-standard base-stations. Techniques for wideband design have been discussed in the literature for frequencies up to 2.6 GHz: for example, in [8] a 20 % fractional bandwidth extension is obtained through a modified Doherty topology requiring a driver module able to properly and separately feed the main and peak stages. A 35 % fractional bandwidth is reported in [9], exploiting wideband filters; in this case a standard topology is adopted, but the Doherty behavior is not clearly demonstrated, and the power utilization factor [4] is not constant in the declared band. Frequency reconfigurable matching networks, enabling for a fractional bandwidth of 20 %, but requiring additional external controls, are proposed in [10]. In [11], the focus is on the use of non-conventional output combining stages, while [12] presents a method applying to broadband matching the simplified real frequency technique. Finally [13] focuses on input direct coupling of main and peak branches and wideband output matching.

This paper proposes a wideband Doherty power amplifier design approach for the 3-3.6 GHz frequency range (18 % bandwidth), adopting a simple technique based on wideband compensators inserted at the output of the peak and main cells. Second-harmonic tuning of the main amplifier [3], [14] has been implemented at the upper bandwidth limit to help gain equalization vs. frequency. The active device exploited in the microstrip hybrid circuit implementation is a packaged GaN HEMT, with typical output power of 10 W in the selected band. The amplifier CW characterization shows, at 6 dB of output power back-off, a drain efficiency between 38 % and 56 % in the 3-3.6 GHz band. In the same range, the amplifier exhibits a maximum output power between 43 dBm and 44 dBm, together with gain around 10 dB.

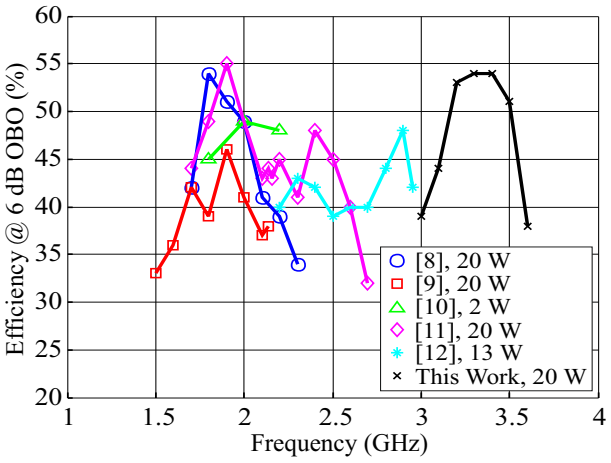

Fig. 1. Efficiency vs. frequency of state-of-the-art wideband Doherty power amplifiers.

J. Moreno Rubio, J. Fang, V. Camarchia, R. Quaglia, M. Pirola, and G. Ghione are with the Department of Electronics and Telecommunications, Politecnico di Torino, C.so Duca degli Abruzzi 24, 10129 Torino, ITALY e-mail: vittorio.camarchia@polito.it

V. Camarchia is also with the Center for Space Human Robotics, Istituto Italiano di Tecnologia, C.so Trento 21, 10129 Torino, ITALY

Fig. 1 compares state-of-the-art results for wideband Doherty power amplifiers: the present work shows high power utilization factor [4], gain flatness, and efficiency in a bandwidth similar to the other sources, but, for the first time according to the authors' knowledge, it exhibits a frequency higher than 3 GHz.

The paper is organized as follows: Section II presents the implemented Doherty design approach and highlights the specific solutions implemented to enlarge the amplifier bandwidth, while Section III illustrates the fabrication, and present the CW characterization results. Some conclusions are drawn in Section IV.

II. Wideband Doherty design strategy

The Doherty PA standard design strategy [3], [4] is well suited to a narrowband amplifier. In fact, the Doherty theory assumes that the main and peak amplifier devices are ideal current generators and exploits an ideal $\lambda/4$ impedance transformer and input power splitter. However, when increasing the amplifier bandwidth, compensation of the main and peak amplifier device output reactance becomes less straightforward; moreover, the impedance transformer, input divider and input matching sections should be in principle made wideband. Additionally, the decreasing intrinsic gain of the device requires to equalize the amplifier gain.

In the present work, we propose a simple method to achieve the proper Doherty modulation on the whole bandwidth while implementing, at the same time, second harmonic tuning [3], [4]. The amount of load modulation and second harmonic tuning are applied as a function of frequency in such a way as to allow for gain equalization on the whole amplifier bandwidth. The selected bandwidth (3.0 to 3.6 GHz) covers the WiMAX 3.5 GHz band as well as part of S-band, that could be adopted in the future for multi-band systems. The employed active device is a commercial packaged GaN HEMT on SiC (CGH40010 from Cree inc.), with typical output power of 10 W in C - band, at 28 V [15] drain bias.

A. Wideband load modulation approach

Direct compensation of the HEMT output reactance becomes less effective when increasing the amplifier bandwidth (Fano's limit [16]). As a consequence, the ideal Doherty behavior is compromised, with negative impact on the expected performances, and actually transforming the Doherty PA into a generic combined module.

In the present approach, we introduce a wideband reactive compensation network cascaded at the output of the main and peak stages, as shown in Fig. 2. The design strategy that is compatible with a simple and compact circuit implementation can be outlined as follows. Ideally, the total scattering matrix $\hat{S}$ (see Fig. 2) of the two-port connecting the intrinsic drain (where the output current generator of the active device is located), to the load should be, on the whole band:

$$\hat{S} = \begin{bmatrix} 0 & \pm 1 \\ \pm 1 & 0 \end{bmatrix} \tag{1}$$

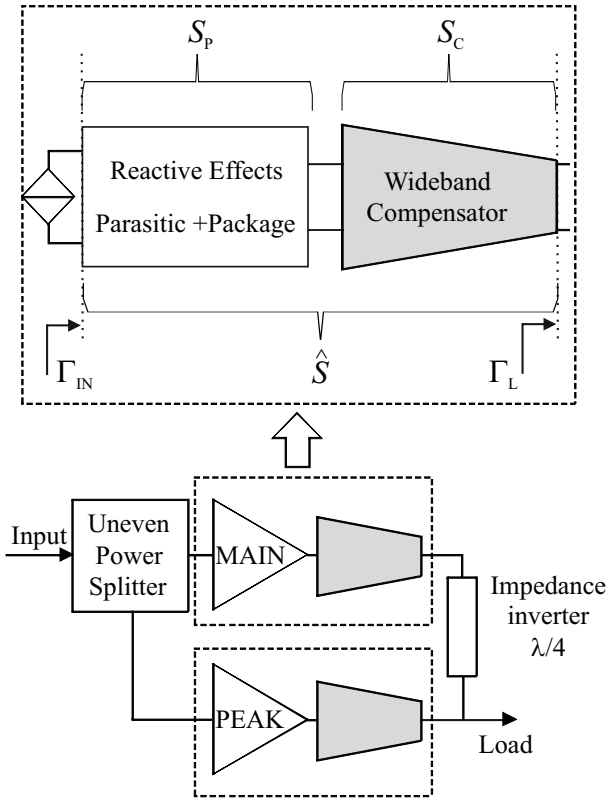

Fig. 2. Block scheme of the proposed wideband Doherty power amplifier.

In fact, (1) implies that the load $\Gamma_{\rm IN}$ seen from the output current generator is equal to $\Gamma_{\rm L}$, see Fig. 2, independent of the reference normalization impedance of $\hat{S}$, since:

$$\Gamma_{\rm IN} = \hat{S}_{11} + \frac{\hat{S}_{21}\hat{S}_{12}\Gamma_{\rm L}}{1 - \hat{S}_{22}\Gamma_{\rm L}} \Rightarrow \Gamma_{\rm IN} = \Gamma_{\rm L}. \tag{2}$$

Assuming negligible losses, the input and output matching condition $\hat{S}_{11} = \hat{S}_{22} = 0$ implies $|\hat{S}_{21}| = |\hat{S}_{12}| = 1$. Condition $\hat{S}_{11} = \hat{S}_{22} = 0$ can be achieved through a wideband matching filter, while a proper delay can be cascaded to adjust the phase of $\hat{S}_{21}$ to obtain $\hat{S}_{21} = \pm 1$ (Fig. 2). In practice, the phase of $\hat{S}_{21}$ was initially imposed at centerband (offset lines lengths of main and peak stages), and then optimized to allow for the proper load modulation of the full Doherty amplifier. Needless to say, conditions $\hat{S}_{11} = \hat{S}_{22} = 0$ and $\hat{S}_{21} = \pm 1$ are only approximately achieved on the whole bandwidth.

The cascade of the wideband matching filter and of the delay line was implemented as follows. We start from the equivalent circuit of the output port of the present active device, including intrinsic and package parasitics, shown in Fig. 3. Denoting as $S_{\rm P}$ the scattering matrix of the reactive L network to be compensated (Fig. 3) and as $\Delta_{S_{\rm P}}$ its determinant, the required input mismatch of the wideband two-port compensator, $S_{11,\rm C}$, can be found to be:

$$S_{11,\rm C} = \frac{S_{11,\rm P}}{\Delta_{S_{\rm P}}} \tag{3}$$

$S_{11,\rm C}$ was obtained from (3) exploiting the equivalent circuit parameters of Fig. 3. Due to the small reactive part of the

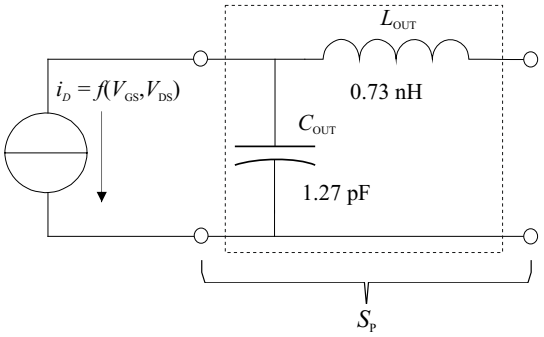

Fig. 3. Cree active device output equivalent circuit model (parasitic + package).

resulting $S_{11,C}$, the real-to-complex transformation from the 50 Ω load is achieved in two steps (see Fig. 4): real-to-real with a wideband two-section transformer, and real-to-complex with an additional transmission line having short electrical length. The two-section transformer is designed according to the method described in [17], and then optimized to obtain the needed bandwidth and ripple performances. An additional delay line (see Fig. 4) is exploited to adjust the total phase according to the condition $\hat{S}_{21} \approx \pm 1$.

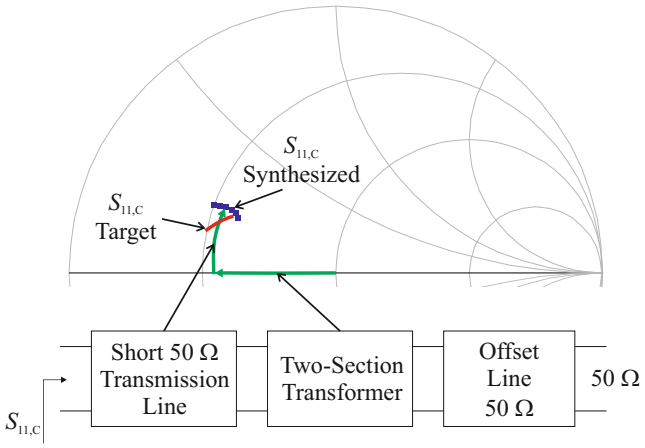

Fig. 4. Optimum and synthesized $S_{11,C}$.

Fig. 4 shows the behavior of the ideal $S_{11,C}$ obtained from (3) in the whole bandwidth for the main stage, (red continuous line), together with the results from the synthesized compensator (blue squares). The simulated $\hat{S}$ (main stage) is reported in Fig. 5; the desired behavior, $\hat{S}_{11} = 0$ and $|\hat{S}_{21}| = 1$, is satisfactorily approximated on the whole amplifier band. Similar results have been achieved for the peak stage compensator.

Concerning the impedance inverter, this is designed as a simple $\lambda/4$ microstrip transmission line. In fact, considering a return loss of 18 dB in the 3-3.6 GHz band (18 %), see Fig. 5, and an impedance transformation ratio of 4, the fractional bandwidth of the $\lambda/4$ inverter results to be 21.5 % [18], hence larger than the one achieved by the output compensators (18 %); resorting to more complex design solutions is therefore not necessary.

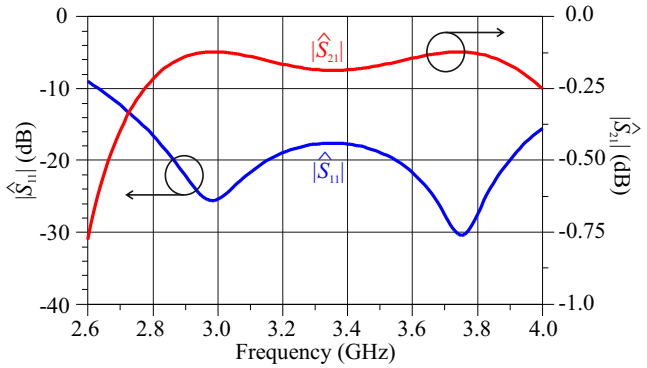

Fig. 5. Simulated behaviour of the $\hat{S}_{11}$, and $\hat{S}_{21}$ of the total scattering matrix connecting intrinsic drain and load of the main stage.

B. Second harmonic tuning and gain equalization

Due to the high breakdown voltage of GaN devices [19], second harmonic tuning [3] can be introduced to increase the efficiency of the main unit with respect to a class B tuned-load stage. Moreover, it can be exploited as an additional tool to equalize the amplifier power gain on the design bandwidth; to this aim, the tuning frequency is set around the upper limit of the band (i.e. above 3.4 GHz, corresponding to lowest gain) by optimizing the lengths of the output offset lines of the main and peak amplifiers, respectively. As a result, the main amplifier behaves as a tuned-load stage in the lower portion of the band, then gradually becomes a second harmonic tuned stage as the frequency reaches the upper limit of the band. The proper terminations for the second harmonic are obtained through the gate and drain bias tee networks. They are realized as a quarter-wave open-circuit stubs at fundamental, which become short circuits at the second harmonic; the stubs can be positioned at an optimized distance from the device terminals with negligible effect on the matching at the fundamental.

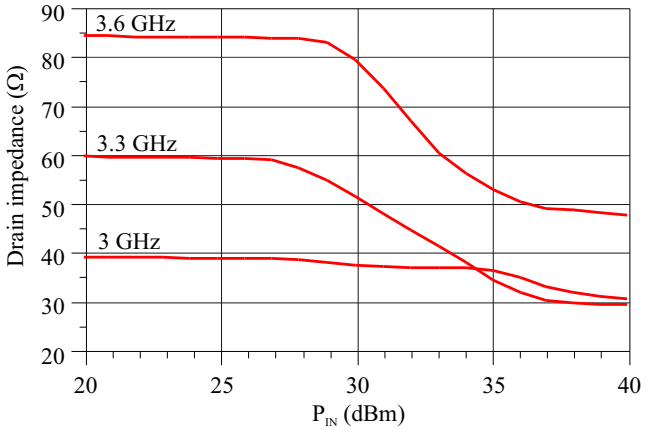

Fig. 6. Load modulation seen from the intrinsic drain of the main device at different frequencies inside the band. Notice that second harmonic tuning is implemented in the upper part of the amplifier bandwidth (opt load 42 Ω), and tuned load in the lower part (opt load 30 Ω).

According to the theory [3], [14], the load impedance corresponding to maximum efficiency is, in the present case, around 30 Ω and 42 Ω for tuned-load condition, and 2nd harmonic tuning, respectively. In Fig. 6, the simulated intrinsic load of the main amplifier is plotted for three frequencies, corresponding to the minimum, maximum, and center of the band, as a function of the output power. As well known from the Doherty theory, the load impedance Z_L at low power should become $Z_L/2$ in power saturation. Such a load modulation is clearly visible in Fig. 6 for the whole amplifier bandwidth. In particular, the load impedance is larger at high frequency, consistent with the second-harmonic tuning strategy (optimum high-power load 42 Ω), while in the lower part of the amplifier bandwidth tuned-load operation is found (optimum high-power load 30 Ω). Notice also, at the lowest end of the amplifier bandwidth, that the load modulation is incomplete, thus playing an additional role in output power equalization.

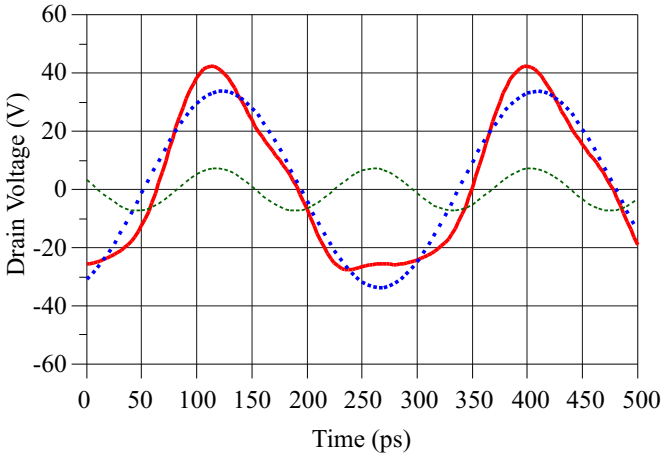

Fig. 7. Main stage: simulated drain voltage waveform (red solid line) centered at 0 V (the constant 28 V DC component was removed) together with its fundamental (blue dotted line) and second harmonic (green dashed line) at 3.5 GHz and 6 dB OBO.

Figs. 7 and 8 show the simulated Doherty drain voltage harmonic components for a 3.5 GHz excitation, at 6 dB output power back-off and at maximum power, respectively. In both cases, second-harmonic tuning increases the maximum swing of the drain voltage without changing the bias condition [14]. Fig. 9 shows the complete schematic of the realized amplifier, also including the wideband source input matching networks at the fundamental, that was designed to minimize the input mismatch in large signal conditions. The input splitter was implemented as a branch-line featuring a small unbalance between the main and peak ports; as for the $\lambda/4$ transformer, the bandwidth achieved with this simple solution was adequate.

III. Realization and Experimental Characterization

The amplifier is fabricated on a Taconic substrate with copper metallization (RF35 with $\epsilon_r = 3.5$, substrate height $H = 0.76$ mm, and metal thickness $t = 0.035$ mm), and mounted on a brass carrier, see Fig. 10. The Doherty amplifier

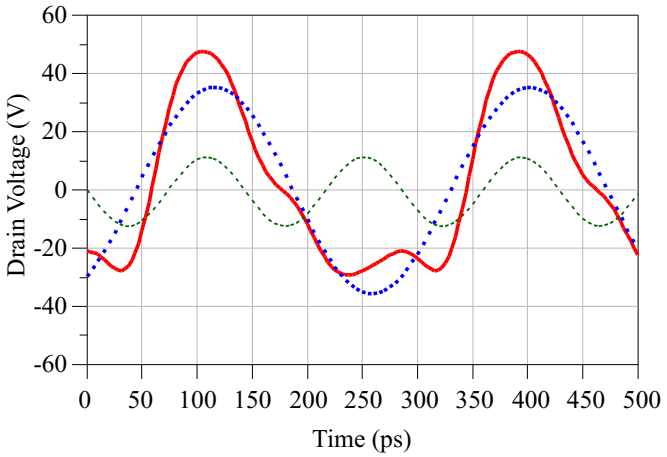

Fig. 8. Main stage: simulated drain voltage waveform (red solid line) centered at 0 V (the constant 28 V DC component was removed) together with its fundamental (blue dotted line) and second harmonic (green dashed line) at 3.5 GHz and full power.

is characterized in DC, small-signal from 2.5 to 4 GHz, and CW single tone excitation from 3 GHz to 3.6 GHz, with 50 MHz step [20], [21]. Fig. 11 shows the comparison between simulated and measured S_{11} and S_{21} in the band from 2.5 to 4 GHz, at $V_{DS} = 28$ V and $V_{GS} = -2.7$ V ($I_{DS} = 200$ mA) for the main, and $V_{DS} = 28$ V and $V_{GS} = -8.4$ V for the peak. The amplifier exhibits a small signal gain higher than 12 dB in the designed frequency band, with return loss better than 10 dB. The good agreement between simulations and measurements, denoted in Fig. 11, has been reached also due to electromagnetic simulations exploited for the most critical microstrip structures, e.g. junctions between strips with very different widths.

The measured drain efficiency and gain of the Doherty amplifier as a function of the output power are shown in

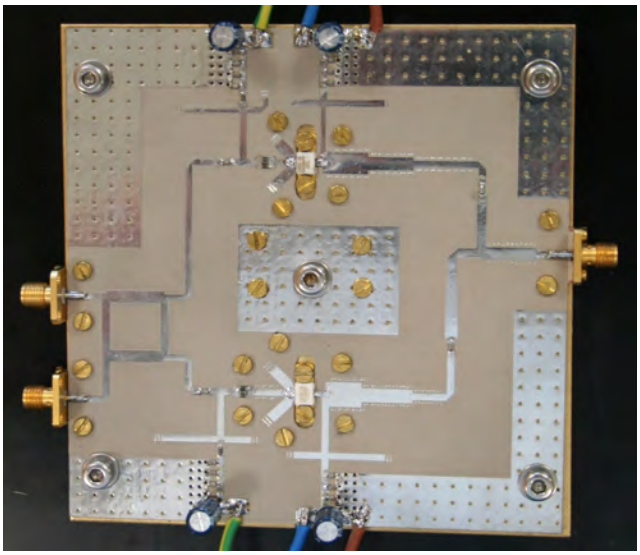

Fig. 10. Picture of the realized wideband Doherty PA.

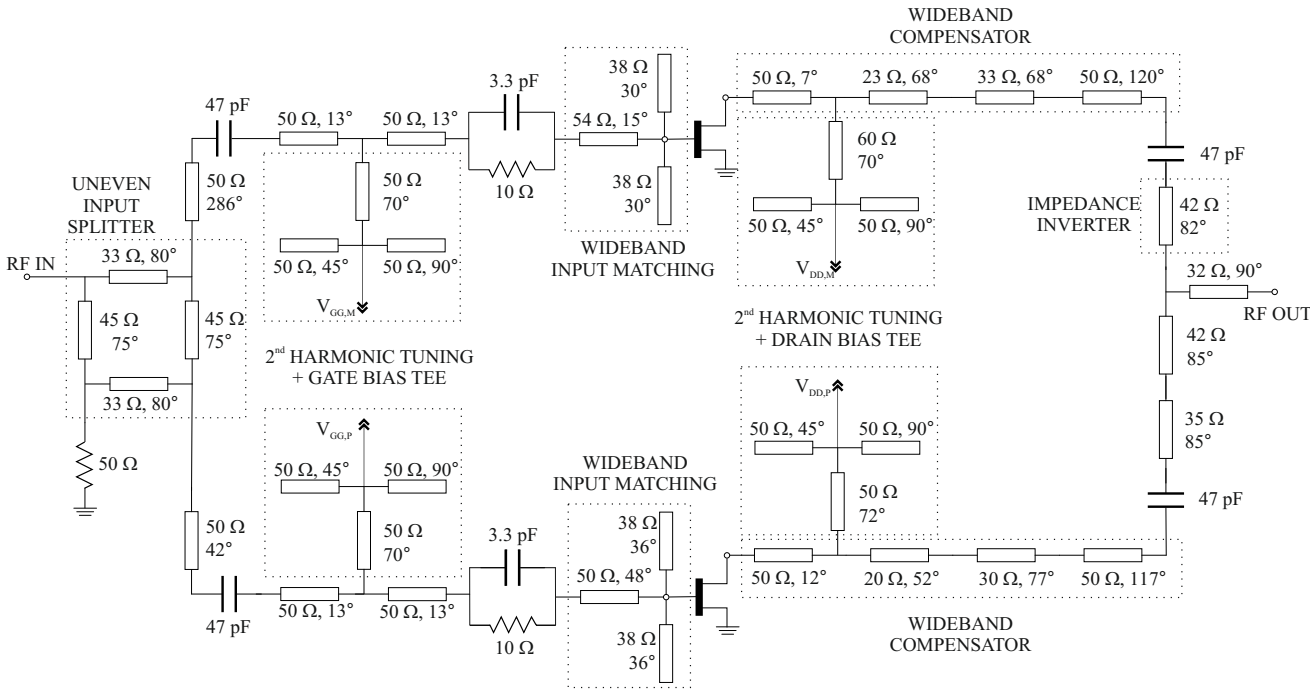

Fig. 9. Complete scheme of the Doherty amplifier. Equivalent ideal lines are represented: electrical lengths refer to center frequency f=3.3 GHz

Fig. 12, for 3.1, 3.3 and 3.5 GHz CW excitation. The typical Doherty high efficiency region can be observed: it spans from a maximum output power exceeding 43 dBm to 6 dB back-off, at all the measurement frequencies. Figs. 13 and 14 plot the maximum output power together with efficiency, and gain respectively, both at maximum output power, and at 6 dB back-off, vs. the excitation frequency. The maximum output power is higher than 43 dBm over the whole band, corresponding to the maximum power utilization factor of the devices, and the gain at 6 dB back-off results well equalized around 10 dB. Regarding the efficiency, it is found to be between 55 % and 66 % at saturation while, at 6 dB back-off, it is between 38 % and 56 %.

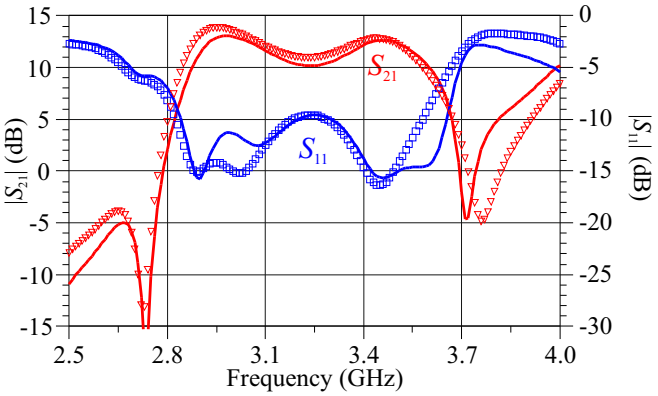

Fig. 11. Comparison between simulated (lines) and measured (symbols) S_{11} (blue), and S_{21} (red) of the Doherty amplifier in the band from 2.5 to 4 GHz, at $V_{DS} = 28$ V and $V_{GS} = -2.7$ V ($I_{DS} = 200$ mA) for the main, and $V_{DS} = 28$ V and $V_{GS} = -8.4$ V for the peak.

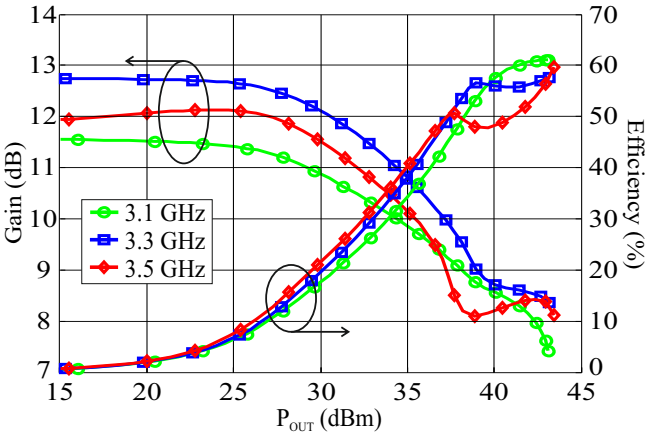

Fig. 12. CW single tone power amplifier characterization at 3.1, 3.3, and 3.5 GHz.

IV. Conclusions

A GaN based wideband Doherty power amplifier has been designed, realized, and characterized in the 3-3.6 GHz frequency band. The design is based on a simple approach that follows the Doherty basic scheme. To obtain wideband behaviour, the output matching networks of the main and peak amplifiers are implemented using wideband compensators. Second harmonic tuning is adopted for the main stage to increase efficiency, and to achieve gain equalization over frequency. An output power exceeding 20 W, together with saturated efficiency over 55 %, and over 38 % at 6 dB back-off are measured; such results favorably compare with the performances of state-of-the-art wideband Doherty amplifiers

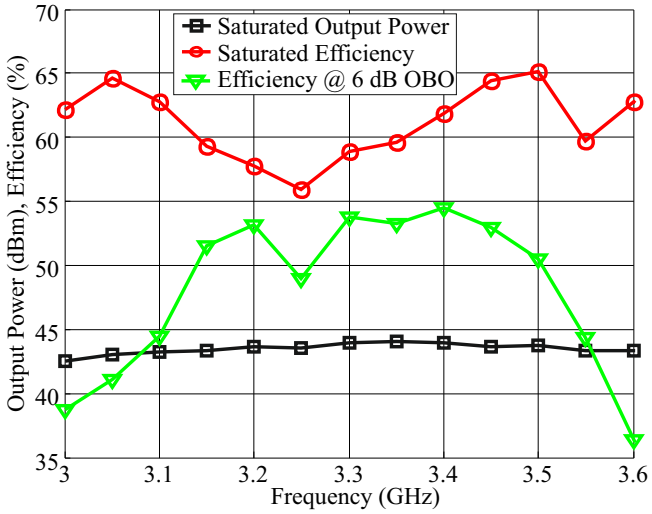

Fig. 13. Power amplifier CW characterization varying excitation frequency. Efficiency at 6 dB OBO and in saturation and saturation output power $vs.$ input power

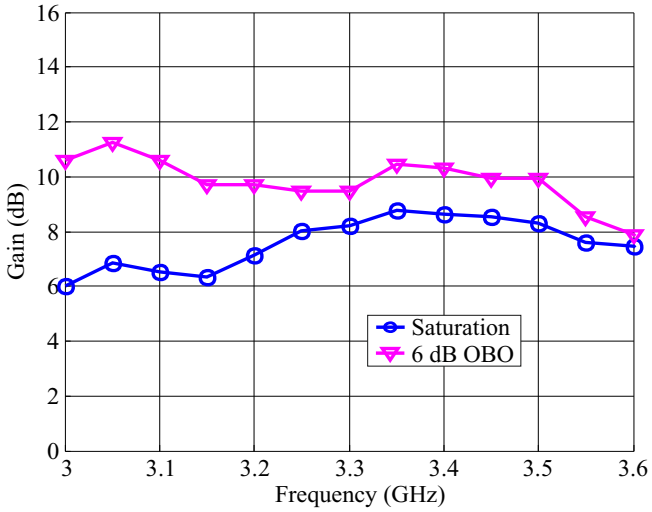

Fig. 14. Power amplifier CW characterization varying excitation frequency. Power gain at 6 dB OBO and in saturation $vs.$ input power

reported in literature.

ACKNOWLEDGMENT

The authors wish to acknowledge the support of the Regione Piemonte NAMATECH project. Prof. Bumman Kim is also acknowledged for his helpful suggestions.

REFERENCES

[1] W. Doherty, "A new high efficiency power amplifier for modulated waves," *Proc. IRE*, vol. 24, no. 9, pp. 1163 – 1182, Sept. 1936.

[2] B. Kim, J. Kim, I. Kim, and J. Cha, "The Doherty power amplifier," *IEEE Microw. Mag.*, vol. 7, no. 5, pp. 42 –50, oct. 2006.

[3] P. Colantonio, F. Giannini, and E. Limiti, *High Efficiency RF and Microwave Solid State Power Amplifiers*, ser. Microwave and Optical Engineering. John Wiley & Sons, 2009.

[4] S. Cripps, *RF power amplifiers for wireless communications*, ser. Artech House Microwave Library. Artech House, 2006.

[5] K.-J. Cho, J.-H. Kim, and S. Stapleton, "A highly efficient Doherty feed-forward linear power amplifier for W-CDMA base-station applications," *IEEE Trans. Microw. Theory Tech.*, vol. 53, no. 1, pp. 292 – 300, jan. 2005.

[6] Y. Yang, J. Cha, B. Shin, and B. Kim, "A fully matched N-way Doherty amplifier with optimized linearity," *IEEE Trans. Microw. Theory Tech.*, vol. 51, no. 3, pp. 986 – 993, mar 2003.

[7] J. Fang, R. Quaglia, J. Rubio, V. Camarchia, M. Pirola, S. Guerrieri, and G. Ghione, "Design and baseband predistortion of a 43.5 dBm GaN Doherty amplifier for 3.5 GHz WiMAX applications," in *Microwave Integrated Circuits Conference (EuMIC), 2011 European*, oct. 2011, pp. 256 –259.

[8] J. Qureshi, N. Li, W. Neo, F. van Rijs, I. Blednov, and L. de Vreede, "A wide-band 20 W LMOS Doherty power amplifier," in *Microwave Symposium Digest (MTT), 2010 IEEE MTT-S International*, may 2010, pp. 1504 –1507.

[9] K. Bathich, A. Markos, and G. Boeck, "A wideband GaN Doherty amplifier with 35 % fractional bandwidth," in *Microwave Conference (EuMC), 2010 European*, sept. 2010, pp. 1006 –1009.

[10] M. Sarkeshi, O. B. Leong, and A. van Roermund, "A novel Doherty amplifier for enhanced load modulation and higher bandwidth," in *Microwave Symposium Digest, 2008 IEEE MTT-S International*, june 2008, pp. 763 –766.

[11] K. Bathich, A. Markos, and G. Boeck, "Frequency response analysis and bandwidth extension of the Doherty amplifier," *IEEE Trans. Microw. Theory Tech.*, vol. 59, no. 4, pp. 934 –944, april 2011.

[12] G. Sun and R. Jansen, "Broadband Doherty power amplifier via real frequency technique," *IEEE Trans. Microw. Theory Tech.*, vol. 60, no. 1, pp. 99–111, jan. 2012.

[13] D. Kang, J. Choi, D. Kim, D. Yu, K. Min, and B. Kim, "30.3% PAE HBT Doherty power amplifier for 2.5–2.7 GHz mobile WiMAX," in *Microwave Symposium Digest (MTT), 2010 IEEE MTT-S International*, may 2010, pp. 796 –799.

[14] J. Rubio, J. Fang, R. Quaglia, V. Camarchia, M. Pirola, S. Guerrieri, and G. Ghione, "A 22W 65% efficiency GaN Doherty Power Amplifier at 3.5 GHz for WiMAX applications," in *Integrated Nonlinear Microwave and Millimetre-Wave Circuits (INMMIC), 2011 Workshop on*, april 2011, pp. 1 –4.

[15] "CGH40010 Rev 3.1, Data Sheet," 2011. [Online]. Available: www.cree.com

[16] R. Fano, "Theoretical limitations on the broadband matching of arbitrary impedances," *Journal of the Franklin Institute*, vol. 249, no. 1, pp. 57 – 83, 1950.

[17] C. Monzon, "A small dual-frequency transformer in two sections," *IEEE Trans. Microw. Theory Tech.*, vol. 51, no. 4, pp. 1157 – 1161, apr 2003.

[18] D. Pozar, *Microwave Engineering, 3rd Ed.* Wiley India Pvt. Limited, 2009.

[19] V. Camarchia, S. D. Guerrieri, M. Pirola, V. Teppati, A. Ferrero, G. Ghione, M. Peroni, P. Romanini, C. Lanzieri, S. Lavanga, A. Serino, E. Limiti, and L. Mariucci, "Fabrication and nonlinear characterization of GaN HEMTs on SiC and sapphire for high-power applications," *Int. J. RF Microw. Comput.-Aided Eng.*, vol. 16, no. 1, pp. 70–80, Jan. 2006.

[20] M. Pirola, V. Teppati, and V. Camarchia, "Microwave measurements Part I: Linear Measurements," *IEEE Instrum. Meas. Mag.*, vol. 10, no. 2, pp. 14 –19, april 2007.

[21] V. Camarchia, V. Teppati, S. Corbellini, and M. Pirola, "Microwave Measurements -Part II Non-linear Measurements," *IEEE Instrum. Meas. Mag.*, vol. 10, no. 3, pp. 34 –39, june 2007.

Jorge Moreno Rubio was born in Villavicencio, Colombia, in 1978. He graduated in electronic engineering from the Universidad Pedagógica y Tecnológica de Colombia, Sogamoso, Colombia, in 2001. He received his Msc. degree in electronic engineering from the Pontificia Universidad Javeriana, Bogotá, Colombia, in 2006. In 2012, he received the PhD. degree in electronic devices from the Politecnico di Torino, Turin, Italy. He is currently a researcher at the Electronics Department of the Universidad Pedagógica y Tecnológica de Colombia (Grupo de Investigación GINTEL, UPTC-COLCIENCIAS). His present research interests concern the design of high efficiency power amplifiers both hybrid and MMIC.

Jie Fang was born in Anging, P.R.China, in 1979. He graduated in electronic engineering from Politecnico di Torino, Turin, Italy in 2009. In 2010, he started the Ph.D. degree in electronic and communications engineering from the Politecnico di Torino, Turin, Italy, working on design and experimental characterization of high efficiency power amplifiers both hybrid and MMIC.

Vittorio Camarchia (S'01-M'04) received the Laurea degree in electronic engineering and the Ph.D. degree in electronic and communications engineering from the Politecnico di Torino, Turin, Italy, in 2000 and 2003, respectively. In 2001, 2002 and 2003 he was a Visiting researcher with the ECE Department, Boston University, Boston, MA, USA. He is currently an Assistant Professor at the Electronics and Telecommunication Department of Politecnico di Torino. His research is focused on RF device modeling, simulation, and characterization, both linear and nonlinear. Dr. Camarchia was the recipient of the 2002 Young Graduated Research Fellowship presented by the Gallium Arsenide application Symposium (GAAS) Association.

Roberto Quaglia was born in Casale Monferrato, Italy, in 1984. He graduated *cum laude* in electronic engineering from Politecnico di Torino in 2008. In 2012, he received the Ph.D. degree in electronic devices from the Politecnico di Torino, Turin, Italy. His present research interests concern the design, modeling and predistortion of high efficiency power amplifiers both hybrid and MMIC. Dr. Quaglia was the recipient of the 2009 Young Graduated Research Fellowship presented by the Gallium Arsenide application Symposium (GAAS) Association.

Marco Pirola (M'97) was born in Velezzo Lomellina, Italy, in 1963. He received the Laurea degree in electronic engineering and the Ph.D. degree from Politecnico di Torino, Italy, in 1987 and 1992 respectively. In 1992 and 1994, he was a Visiting Researcher at the Hewlett Packard Microwave Technology Division, Santa Rosa, CA. Since 1992, he has been with the Electronic Department of Politecnico di Torino, first as researcher and, since 2000, as associate professor, where his research concerns the simulation, modeling and measurements of microwave devices and systems.

Giovanni Ghione (M'87-SM'94-F'07) was born in 1956 in Alessandria, Italy. He graduated *cum laude* in electronic engineering from Politecnico di Torino in 1981. In 1990 he joined the University of Catania as Full Professor of Electronics, and since 1991 he has covered the same position again at Politecnico di Torino, II Faculty of Engineering. His present research interests concern the physics-based simulation of active microwave and optoelectronic devices, with particular attention to noise modeling, thermal modeling, active device optimization. His research interests also include several topics in computational electromagnetics, including coplanar component analysis. He is Associate Editor of the IEEE ED Transactions, member of the Editorial Board of the IEEE MTT Transactions, Fellow of the IEEE and member of the AEI (Associazione Elettrotecnica Italiana).